STAR Protocols

CellPress
OPEN ACCESS

Protocol

Synthesis and characterization of highly diluted polyanionic iron(II) spin crossover systems

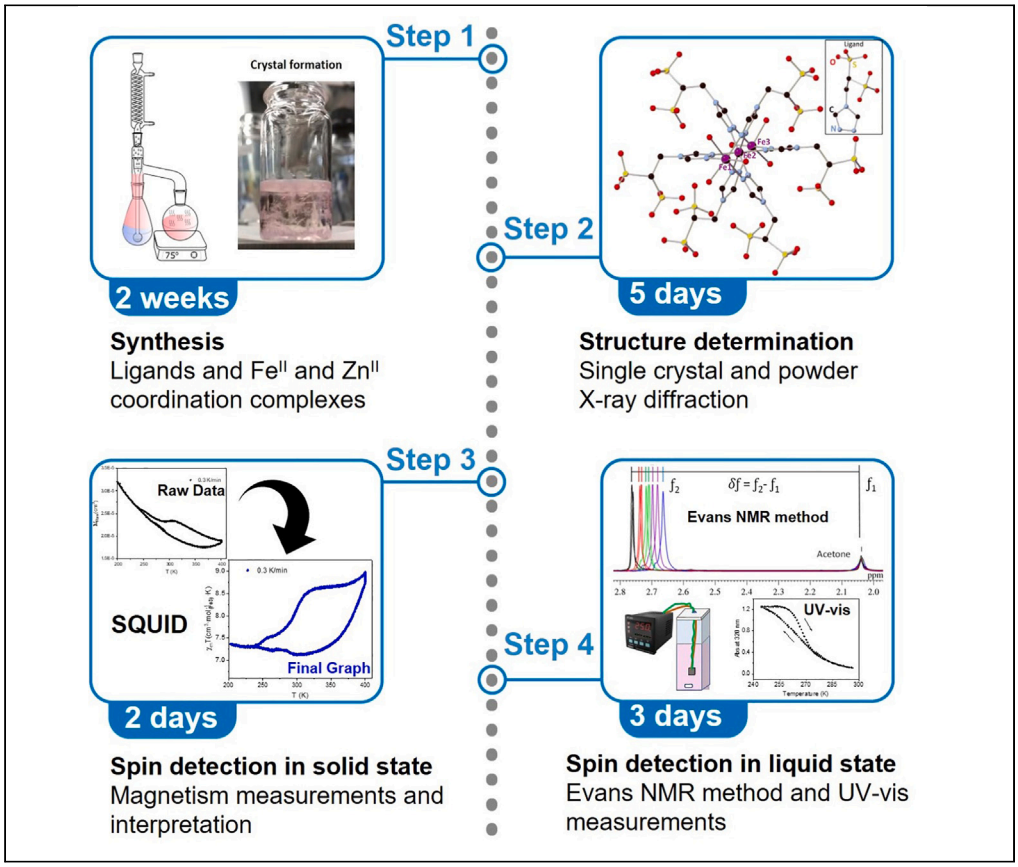

Spin crossover (SCO) complexes, through their reversible spin transition under external stimuli, can work as switchable memory materials. Here, we present a protocol for the synthesis and characterization of a specific polyanionic iron SCO complex and its diluted systems. We describe steps for its synthesis and the determination of crystallographic structure of the SCO complex in diluted systems. We then detail a range of spectroscopic and magnetic techniques employed to monitor the spin state of the SCO complex in both diluted solid- and liquid-state systems.

Publisher's note: Undertaking any experimental protocol requires adherence to local institutional guidelines for laboratory safety and ethics.

Andrea Moneo-Corcuera, David Nieto-Castro, Jordi Cirera, ..., Mónica Helvia Pérez-Temprano, Eliseo Ruiz, José Ramón Galán-Mascarós

moneocorcueraandrea@gmail.com (A.M.-C.)
dnieto@cidetec.es (D.N.-C.)
jrgalan@iciq.es (J.R.G.-M.)

Highlights

Synthesis of diluted systems based on spin crossover (SCO) Fe II trimer

Crystallographic structure determination of SCO systems

Magnetic studies of SCO complexes highly diluted in a diamagnetic matrix

Strategies to follow the spin transition of SCO complexes in solution

Moneo-Corcuera et al., STAR Protocols 4, 102394 September 15, 2023
https://doi.org/10.1016/j.xpro.2023.102394

STAR Protocols

CellPress
OPEN ACCESS

Protocol

Synthesis and characterization of highly diluted polyanionic iron(II) spin crossover systems

Andrea Moneo-Corcuera,[1,8,9,*] David Nieto-Castro,[1,8,9,*] Jordi Cirera,[2] Verónica Gómez,[1] Jesús Sanjosé-Orduna,[1] Carla Casadevall,[1,3] Gábor Molnár,[4] Azzedine Bousseksou,[4] Teodor Parella,[5] José María Martínez-Agudo,[6] Julio Lloret-Fillol,[1,7] Mónica Helvia Pérez-Temprano,[1] Eliseo Ruiz,[2] and José Ramón Galán-Mascarós[1,7,9,*]

[1]Institute of Chemical Research of Catalonia (ICIQ), The Barcelona Institute of Science and Technology (BIST), Av. Països Catalans 16, 43007 Tarragona, Spain

[2]Departament de Química Inorgànica i Orgànica and Institut de Química Teòrica i Computacional, Universitat de Barcelona, Diagonal 645, 08028 Barcelona, Spain

[3]Department of Physical and Inorganic Chemistry, University Rovira i Virgili (URV), C/ Marcel.lí Domingo, 1, 43007 Tarragona, Spain

[4]LCC, CNRS & University of Toulouse (UPS, INPT), 205 route de Narbonne, 31077 Toulouse, France

[5]Servei de Ressonància Magnètica Nuclear, Universitat Autònoma de Barcelona, Bellaterra, 08193 Barcelona, Spain

[6]Instituto de Ciencia Molecular, Universidad de Valencia, Catedrático José Beltrán 2, 46980 Paterna, Spain

[7]ICREA, Passeig Lluís Companys, 23, 08010 Barcelona, Spain

[8]Technical contact

[9]Lead contact

*Correspondence: moneocorcueraandrea@gmail.com (A.M.-C.), dnieto@cidetec.es (D.N.-C.), jrgalan@iciq.es (J.R.G.-M.)
https://doi.org/10.1016/j.xpro.2023.102394

SUMMARY

Spin crossover (SCO) complexes, through their reversible spin transition under external stimuli, can work as switchable memory materials. Here, we present a protocol for the synthesis and characterization of a specific polyanionic iron SCO complex and its diluted systems. We describe steps for its synthesis and the determination of crystallographic structure of the SCO complex in diluted systems. We then detail a range of spectroscopic and magnetic techniques employed to monitor the spin state of the SCO complex in both diluted solid- and liquid-state systems.

For complete details on the use and execution of this protocol, please refer to Galán-Mascaros et al.[1]

BEFORE YOU BEGIN

Spin-crossover (SCO) materials are switchable transition metal complexes where the ground low-spin (LS) and the excited high-spin (HS) state can be reversibly interconverted by external stimuli (temperature, light, pressure, magnetic field, etc.).[2–6] In particular, iron(II) SCO complexes show a dramatic change upon LS ⇔ HS transition in the magnetic properties (from diamagnetic S = 0 to paramagnetic S = 2 in octahedral Fe(II) centers), also in color (from pink/red to white/yellow) and size (increment of 10%–15% in the metal to ligand bonding distances).[7] When the thermally-induced SCO complexes are in the solid state, the spin transition can describe a thermal hysteresis loop, conferring a memory effect to these materials with potential application as a magnetic memories.[8–10] This thermal hysteresis is typically a result of cooperative intermolecular interactions among a large network of active SCO molecules, associating the spin transition to a crystallographic phase transition.[11–13] Previous studies of common hysteretic SCO complexes immersed in non-active SCO matrix confirmed the role of the cooperative interactions in the memory effect, since

the thermal hysteresis dissapear upon relatively low dilution.[14,15] In contrast to these complexes, recent studies of a particular polyanionic iron trimer show memory effects upon highly diluted systems in solid and liquid state.[1] The spin transition detection of highly-diluted SCO systems requires specific characterization techniques and further experimental optimization.

The protocol below can be divided in a synthetic and characterization section. Here, we describe the synthesis of the polyanionic Fe(II) SCO complex $[Fe_3(\mu\text{-}L)_6(H_2O)_6]^{6-}$ (L^{2-} = 4-(1,2,4-triazol-4-yl) ethanedisulfonate (**Fe_3**) and its dilution in a diamagnetic matrix (Fe_3 is diluted with its diamagnetic, isomorphous Zn(II) analogous (**Zn_3**)). In the characterization protocol, we present the specific experimental conditions and the optimized parameter in multiple spectroscopic and magnetic techniques capable to monitor the spin transition. The synthesis protocol can be applied for the coordination of other Fe(II) ions with organic ligands and the immersion of any complex in a diamagnetic matrix. The characterization techniques are capable of precisely monitoring the spin transition of any highly diluted SCO system.

KEY RESOURCES TABLE

REAGENT or RESOURCE	SOURCE	IDENTIFIER
Chemicals, peptides, and recombinant proteins		
N,N-Dimethylformamide (DMF)	Iris Biotech	68-12-2
Thionyl chloride ($SOCl_2$)	Merck (sigma)	7719-09-7
Hydrazine hydrate 64-65 ($NH_2NH_2 \cdot H_2O$)	Aldrich	7803-57-8
Diethyl ether	Aldrich	60-29-7
Ethanol (99.8%)	Vidrafoc	64-17-5
Sodium carbonate anhydrous (Na_2CO_3)	Cymit	497-19-8
Acrylic acid, anhydrous (99%), 200 ppm MEHQ	Sigma	79-10-7
Sulfuric acid fuming (with 30% of fuming SO_3)	Aldrich	8014-95-7
Ammonium 2-aminoethane-1,1-disulfonic acid hydrate	abcr	1235825-84-9
Iron (II) perchlorate heptahydrate	Sigma	335159-18-7
L(+)-Ascorbic acid	Aldrich	50-81-7
Zinc (II) perchlorate hexahydrate	Cymit	10025-64-6
Ethylene glycol	Merck	107-21-1
Methanol-d4	Merck	811-98-3
Deuterium oxide, 99.9%	Merck	7789-20-0
Deposited data		
Crystallographic data: $(Me_2NH_2)_6[(Fe_3(L)_6(H_2O)_6$	CCDC	CCDC: 1016539
Crystallographic data: $(Me_2NH_2)_6[(Zn_3(L)_6(H_2O)_6$	CCDC	CCDC: 2019876
Other		
Diffractometer for SCXRD	Bruker	APEX duo
Diffractometer for PXRD	Siemens	D5000
Magnetometer	Quantum Design	MPMS-XL SQUID
NMR spectrometer	Bruker	500 and 600 MHz
UV-Vis spectrophotometer	Agilent	8453 diode array
SHELXTL	SCXRD software	https://software.pan-data.eu/software/134/shelx
FullProf	PXRD software	https://www.ill.eu/sites/fullprof/php/downloads.html

STEP-BY-STEP METHOD DETAILS

Synthesis of the triazol-based ligand $(Me_2NH_2)_2L$)

Timing: 7 days

The synthesis of the ligand (dimethyl-ammonium 4-(1,2,4-triazol-4-yl) ethanedisulfonate) is divided in four main synthetic steps.

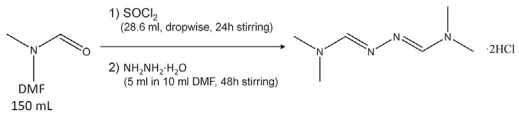

Scheme 1. Synthesis of N,N-dimethylformamide azine dihydrochloride

1. Synthesis of N,N-dimethylformamide azine dihydrochloride.
   a. Add 150 mL of DMF to a 250 mL three-neck round bottom flask and introduce it into an ice bath.
   b. After cooling down for 15 min, add dropwise 28.6 mL of $SOCl_2$ (0.4 mol) to the DMF under stirring and with the necks covered.
   c. Stir the solution for 24 h.
   d. Slowly add 5 mL of $NH_2NH_2 \cdot H_2O$ (0.1 mol) to 10 mL of DMF and stir for 5 min.
   e. Introduce the three-neck round bottom flask into bath ice and add dropwise the previous solution. The scheme of the reaction is shown in Scheme 1.
   f. Stir for 48 h.
   g. Filter the yellow precipitate and wash it 3 times with DMF and 3 times with ethanol and diethyl ether and dry it under vacuum.
   h. Analyze the product by ^{1}H NMR (300 MHz, D_2O): δ = 8.4 ppm (s, 1 H), δ = 3.4 ppm (broad peak, 6 H). Ethanol peaks might be observed: δ = 3.7 ppm (t), δ = 1.25 ppm (t).[16]

⚠ CRITICAL: These reactions are very exothermic. All the steps must be carried out in a fume hood. The filtration of the product must be performed in a Fritted glass (not paper filter).

2. Preparation of N,N-Dimethylformamide Azine.
   a. Dissolve 20.5 g of N,N-dimethylformamide azine dihydrochloride (0.1 mol) in 100 mL of H_2O.
   b. In a different beaker, dissolve 10.6 g of Na_2CO_3 (0.1 mol) in 100 mL of H_2O.
   c. Slowly mix both solutions in a round bottom flask (Na_2CO_3 solution on top of the azine solution), Scheme 2.
   d. Extract the N,N-Dimethylformamide Azine via liquid-liquid extraction with 750 mL of diethyl ether at 50°C for 48 h (See Figure 1 for liquid-liquid extraction set-up and scheme of the reaction).
   e. Concentrate the organic layer in vacuum until obtaining an orange powder.
   f. Analyze the product by ^{1}H NMR (300 MHz, D_2O): δ = 8.4 ppm (s, 1 H), δ = 3.4 ppm (s, 6 H).

⚠ CRITICAL: These steps must be carried out in a fume hood because H_2CO_3 gas is generated when Na_2CO_3 is added to N,N-dimethylformamide azine dihydrochloride and for the volatile diethyl ether.

3. Synthesis of 2-aminoethane-1,1-disulfonic acid (Optional).
   a. Add 6.85 mL of acrylic acid (0.1 mmol) and 15 mL of acetonitrile into a 500 mL three-necked bottom flask placed in an ice bath.
   b. Dropwise add 40 mL of fuming sulfuric acid (25% SO_3) and stir for 30 min.
   c. When the solution is cooled down at room temperature (20°C–25°C), reflux the solution at 100°C for 1 h.
   d. Stir overnight (10–14 h) at room temperature (20°C–25°C).

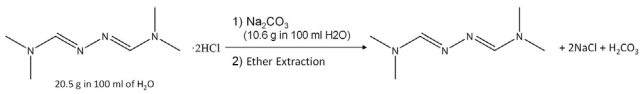

Scheme 2. Neutralization of N,N-dimethylformamide azine

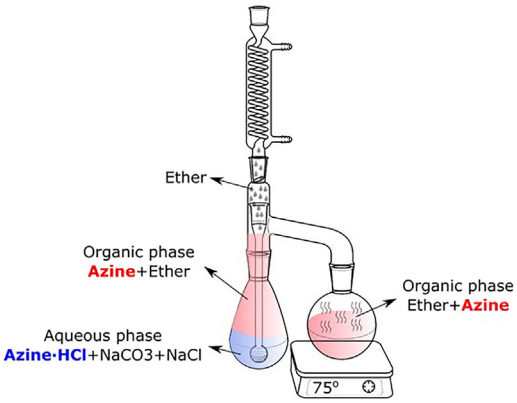

Figure 1. Set up for the neutralization of N,N-dimethylformamide azine dihydrochloride
The organic phase extracts correspond to the neutral azine from the aqueous solution.

e. The next day, place the bottom flask in an ice bath and add 85 mL of H_2O.
f. Reflux the solution at 100°C for 24 h.
g. Place the round flask in the fridge for 48 h, see reaction in Scheme 3.
h. Filter and wash with H_2O, Ethanol and diethyl ether.
i. Analyze the product by ^{1}H NMR (300 MHz, D_2O): δ = 4.3 (t, 1 H), δ = 3.6 (t, 2 H). Ethanol peaks might be observed: δ = 3.7 (t), δ = 1.3 (t).[17]

⚠ CRITICAL: The fuming sulfuric acid (25% SO_3) reagent generates high amount of SO_3 vapors, and it should be opened in the fume hood. The reaction between the sulfuric acid (25% SO_3) and the acrylic acid/acetonitrile mixture is highly exothermic, resulting in a rapid and locally temperature increase. Small explosion can be produced. Be sure the set-up is secure.

Note: The 2-aminoethane-1,1-disulfonic acid is also commercial, see key resources table.

4. Synthesis of Dimethyl-ammonium 4-(1,2,4-triazol-4-yl)ethanedisulfonate) ($(Me_2NH_2)_2L$).
a. Dissolve 3.0 g of N,N-Dimethylformamide Azine (21.0 mmol) to 20 mL of H_2O into a 50 mL round bottom flask.
b. Add 2-aminoethane-1,1-disulfonic acid (1.5 g, 7.0 mmol) to the previous solution.
c. Add HCl until pH = 6.
d. Reflux the solution at 95°C for 19 h.
e. Remove the solvent under vacuum, obtaining a yellow oil.
f. Add 40 mL of ethanol to allow precipitation and keep the solution in the fridge overnight (10–14 h). See complete reaction in Scheme 4.
g. Filter the white powder, wash it with diethyl ether and dry it open air.
h. Analyze the product by ^{1}H NMR (300 MHz, D_2O): δ = 4.8 (s, 2 H), δ = 2.8 (s, 6 H).[17]

Synthesis of Fe^{II} and Zn^{II} coordination complexes

Timing: 7 days

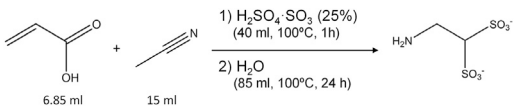

Scheme 3. Synthesis of 2-aminoethane-1,1-disulfonic acid

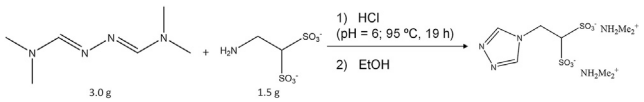

Scheme 4. Synthesis of $Me_2NH_2)_2L$

The coordination of the ligand (dimethyl-ammonium 4-(1,2,4-triazol-4-yl) ethanedisulfonate) to Fe and Zn ions lead to the formation of linear trimers with formula $(Me_2NH_2)_6[(M_3(L)_6(H_2O)_6)]$ (M = Fe or Zn).

5. Synthesis of $(Me_2NH_2)_6[(Fe_3(L)_6(H_2O)_6)]$ (**Fe_3**).
   a. Dissolve 0.1 g of $Fe(ClO_4)_2 \cdot 6H_2O$ (0.35 mmol) and a small amount of ascorbic acid in 5 mL of H_2O.
   b. Dissolve 0.3 g of $(Me_2NH_2)_2L$ (0.87 mmol) in 5 mL of H_2O.
   c. Mix the two solutions for 15 min, obtaining a pale pink solution.
   d. For the obtention of a polycrystalline powder:
      i. Add 20 mL of ethanol, leading to the precipitation of a pink solid.
      ii. Centrifuge the suspension (1900 × *g*) and decant the supernatant liquid.
      iii. Wash three times with ethanol.
      iv. Dry at 60°C for 2 h, see product in Figure 2.
      v. Analyze the product via Powder X-ray diffraction in the 5−40° 2θ range. See next section, entitled: Structure of Fe^{II} and Zn^{II} coordination complexes).
   e. For the obtention of crystals:
      i. Add 3 mL of the solution from section 5c) to a 5 mL glass vial.
      ii. Introduce the vial into a 50 mL glass vial.
      iii. Add ethanol in the outer space until the level of ethanol is higher than the inner solution (See Figure 3, left) and close the 50 mL vial (seal it with parafilm).
      iv. Pink needle shaped crystals are obtained after 3–5 days at room temperature (20°C–25°C) (See Figure 3, right).
      v. Analyze the crystals via single crystal X-ray diffraction (SCXRD). See next section, entitled: Structure of Fe^{II} and Zn^{II} coordination complexes.
6. Synthesis of $(Me_2NH_2)_6[(Zn_3(L)_6(H_2O)_6)]$ (**Zn_3**).
   The synthesis protocol for **Zn_3** is analogue to **Fe_3** synthesis.
   a. Dissolve 0.12 g of $Zn(ClO_4)_2 \cdot 6H_2O$ (0.1 mmol) in 5 mL of H_2O.
   b. Dissolve 0.3 g of $(Me_2NH_2)_2L$ (0.87 mmol) in 5 mL of H_2O.
   c. Mix the two solutions for 15 min, obtaining white solution.
   d. For the obtention of a polycrystalline powder:
      i. Add 20 mL of ethanol, leading to the precipitation of a white solid.
      ii. Centrifuge the suspension (1900 × *g*) and decant the supernatant liquid.
      iii. Wash three times with ethanol.
      iv. Dry at 60°C for 2 h.
      v. Analyze the powder via Powder X-ray diffraction in the 5−40° 2θ range.
   e. For the obtention of crystals:
      i. Add 3 mL of the solution from section 6diii to a 5 mL glass vial.

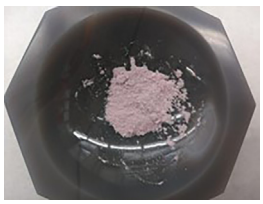

Figure 2. Picture of the powder of Fe_3

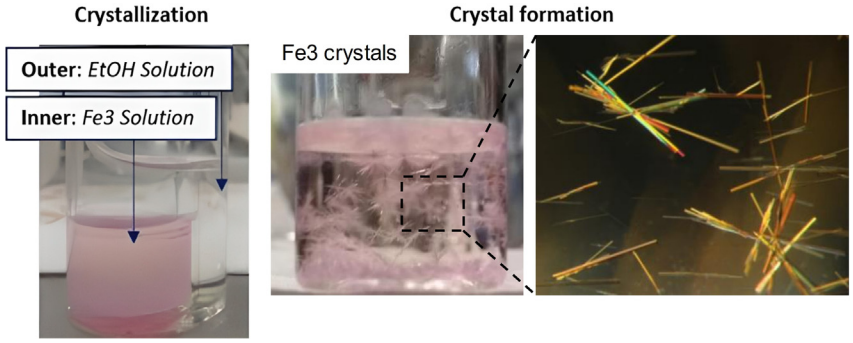

Figure 3. Pictures of the ethanol vapor slow diffusion technique for obtaining Fe_3 crystals

ii. Introduce the vial into a 50 mL glass vial.
iii. Add ethanol in the outer space until the level of ethanol is higher than the inner solution and close the 50 mL vial (seal it with parafilm).
iv. Crystals are obtained after 3–5 days at room temperature (20°C–25°C).
v. Analyze the crystals via single crystal X-ray diffraction (SCXRD). See next section, entitled: Structure of Fe^{II} and Zn^{II} coordination complexes).

7. Synthesis of solid dilution $Zn_{3(1-x)}Fe_{3(x)}$.
   a. Dissolve the desired molar ratio of Fe_3 and Zn_3 (Table 1) and 20 mg of $(Me_2NH_2)_2L$ in 10 mL of H_2O with ascorbic acid.
   b. Stir for 15 min.
   c. Add 20 mL of ethanol, obtaining a suspension.
   d. Centrifuge the suspension (1900 × *g*) and collect the solid.
   e. Wash the solid with ethanol and dry it in air.
   f. The actual Fe/Zn content was determined by EDX and ICP-OES (inductive coupled plasma optical emission spectroscopy) analysis (see values in Table 2).
   g. Analyze the powder via Powder X-ray diffraction in the 5−40° 2θ range. See next section, entitled: Structure of Fe^{II} and Zn^{II} coordination complexes).

Structure of Fe^{II} and Zn^{II} coordination complexes

Timing: 5 days

The crystallographic structure of Fe^{II} and Zn^{II} complexes can be determined by combining single crystal and powder X-ray diffraction.

Single-crystal X-Ray diffraction (SCXRD)

8. Collect Single-Crystal X-Ray diffraction (SCXRD) data at 100 K with a diffractometer, Bruker APEX duo diffractometer with an APEX II CCD detector using Mo-Ka (λ = 0.71073 Å) and equipped with an Oxford Cryostrem 700 plus.
9. Obtain the crystal structure solution using SHELXTL and the XP program.

Table 1. Amounts of Fe_3 and Zn_3 used to form the solid dilutions $Zn_{3(1-x)}Fe_{3(x)}$

x	mg Fe_3	mmol Fe_3	mg Zn_3	mmol Zn_3
0.60	29.6	0.013	20.0	0.009
0.40	19.7	0.009	30.0	0.013
0.20	9.9	0.004	40.0	0.018
0.05	2.5	0.001	47.5	0.021

Table 2. Estimation of x in the $Zn_{3(1-x)}Fe_{3(x)}$ series by EDX and ICP-OES data

	EDX	ICP-OES
x	x_{found}	x_{found}
0.60	0.540	0.520
0.40	0.360	0.320
0.20	0.190	0.160
0.05	0.055	0.045

Note: Both structures crystallized with high degree of disorders with one molecule of an anionic trimetalic complex, six dimethylammonium cations and five water molecules in the asymmetric unit, being Fe3 and Zn3 isostructural complexes (Figure 4). (Fe_3 CCDC deposition number: 1016539 ; Zn3 CCDC deposition number: 2019876).

Powder X-ray diffraction (PXRD)

10. Perform PXRD to the $Zn_{3(1-x)}Fe_{3(x)}$ solid dilutions in order to confirm the absence of local phase separation. In our case we used a Siemens D5000 diffractometer fitted with a curved graphite diffracted-beam monochromator, incident, and diffracted-beam Soller slits, a 0.06° receiving slit and scintillation counter as a detector. Parameters of the sequence:
    a. 2θ range: 5°–40°.
    b. Angular step: 0.05° at 10 s per step and sample rotation.
    c. Radiation source: Cu-kα from a copper X-ray tube operated at 40 kV and 30 mA.
11. Analise the PXRD patterns via Pawley profile refinement (Figure 5) or via LeBail refinement. These refinements can be performed using TOPAS software or the open access FullProf software.

Spin transition detection of the iron trimer (Fe_3) in $Zn_{3(1-x)}Fe_{3x}$

Timing: 2 days

Magnetic measurements

The magnetic properties of the solid samples are measured via a superconducting quantum interference devices (SQUID) magnetometer. In this case, we used a Quantum Design MPMS-XL SQUID magnetometer (Quantum Design, San Diego, CA, USA) under a 1000 Oe field.

12. Sample preparation:
    a. Weight an open gel capsule. Write the weight change in each following steps.

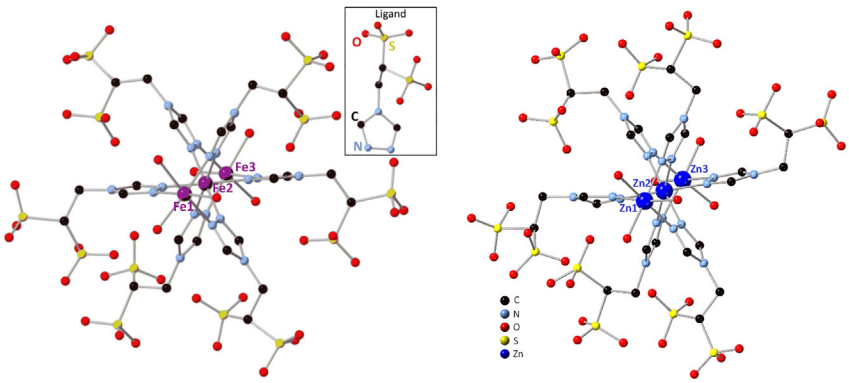

Figure 4. Representation of the molecular structure of Fe_3 (left) and Zn_3 (right)
Hydrogen atoms were omitted for clarity.

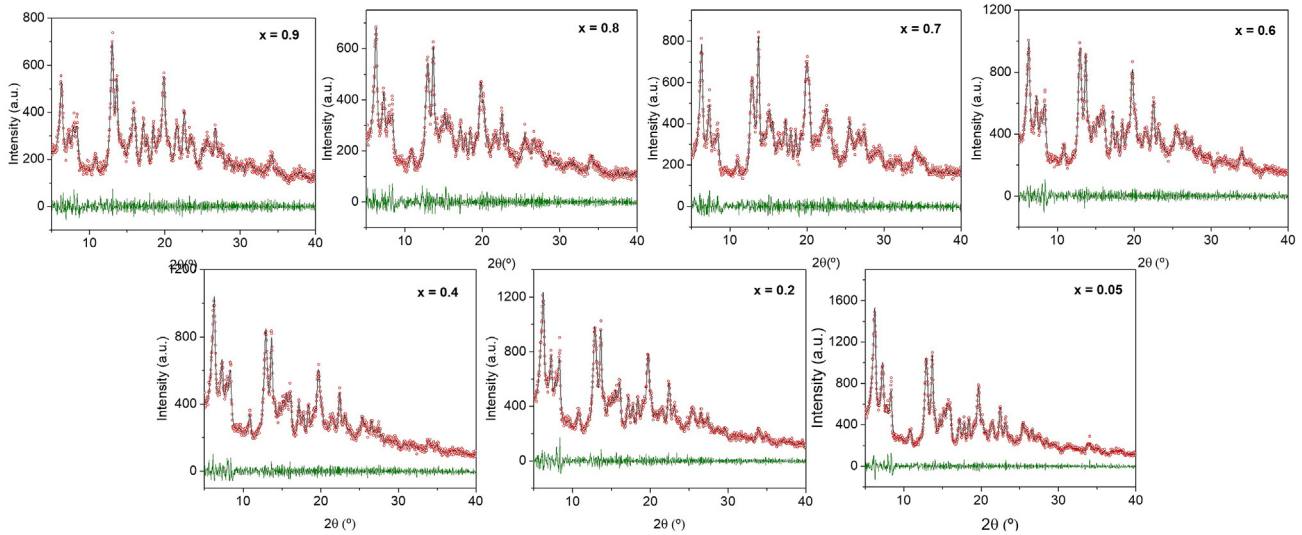

Figure 5. Pawley refinement (black line) of PXRD patterns (red circles) for $Zn_{3(1-x)}Fe_{3(x)}$

The green line represents the difference between fitting and experimental data.

b. Fill the capsule with approximately 35 mg of the homogeneous powder. Introduce glass wool or cotton in the capsule.
c. Close the capsule with Kapton tape (Figure 6 **bottom**).
d. Make a 1 mm diameter hole in the top part of the capsule to facilitate the purge inside the capsule and allow the sample dehydration during the first heating process.
e. Introduce the capsule in a plastic straw (Figure 6 **top**) and place it in the sample holder of the magnetometer.

13. For magnetic measurements, use the PPMS *MultiVu* software in RSO mode to create a sequence of 5 cycles at 1000 Oe between 200 and 400 K with different scan rates (2 K/min – 0.3 K/min).
14. Data treatment.
    a. From the raw magnetization data (Figure 7A), correct the diamagnetic contribution of the sample holder (capsule and glass glow/cotton), obtaining the net magnification (Figure 7B). For this, use the following equations:

$$M_{net} = M_{raw} - M_{bag} - M_{wool}$$

$$M_{bag} = H \cdot m(bag) \cdot \left(-2.0188 \cdot 10^{-4} \cdot H - 2.63066 + \frac{2.96773}{T} \right) 10^{-10}$$

$$M_{wool} = H \cdot m(wool) \cdot \left(\frac{3.0461}{T} \right) 10^{-8}$$

Where M is the magnetization (cm^3) of the sample (M_{net}) and sample holder (M_{bag} and M_{wool}), H is the magnetic field (Oe) and m is the mass (mg).

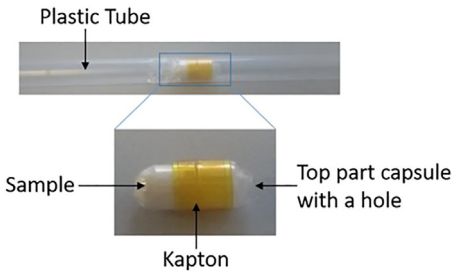

Figure 6. Picture of the sample ready to measure in the SQUID

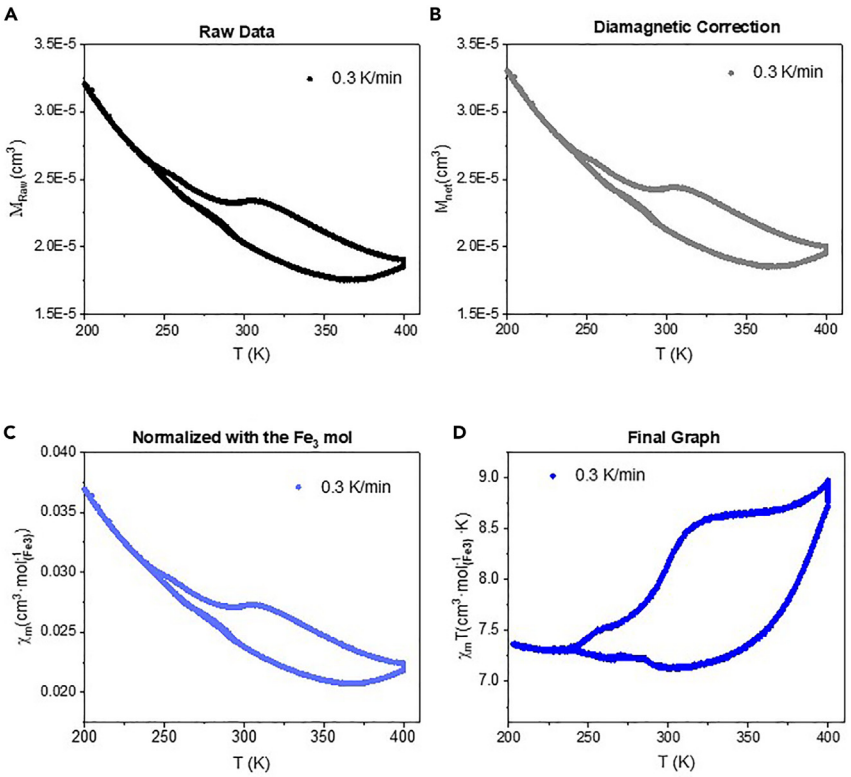

Figure 7. Data correction process for magnetic susceptibility cycle of $Zn_{3(1-x)}Fe_{3(x)}$ (x = 0.4)

(A) Raw magnetization extracted from the SQUID measurements. (B) Net magnetization obtained after correction of the diamagnetic contribution of the sample holder. (C) Magnetization per mol of iron trimer. (D) Final graph representing magnetic susceptibility temperature product ($X_m \cdot T$) vs. temperature.

b. After this first correction, use the following equation to represent the magnetization per mol of iron trimer (Figure 7C):

$$\chi_M = \frac{(M - M_{bag} - M_{wool}) \cdot M_m}{m(Fe_3) \cdot H}$$

Where X_M is the molar magnetic susceptibility of the sample (cm^3·mol^{-1}) and M_m is the molecular weight of the **Fe_3** complex (2191.6 mg mmol^{-1}).

c. Finally, represent the magnetic susceptibility temperature product ($X_m \cdot T$) vs. temperature, Figure 7D.

15. Magnetic data interpretation.

a. Compare the experimental magnetic susceptibility data with the theoretical $\chi_M T$ values for an iron^{II} trimer with two different configurations ($Fe^{II}_{HS}Fe^{II}_{LS}Fe^{II}_{HS}$ and $Fe^{II}_{HS}Fe^{II}_{HS}Fe^{II}_{HS}$).

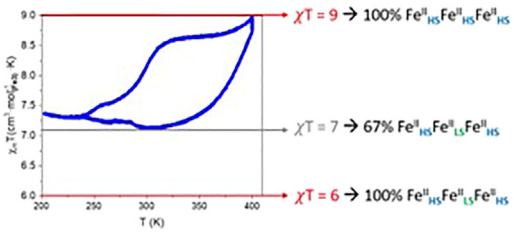

Figure 8. Magnetic susceptibility data in the 200–400 K range for $Zn_{3(1-x)}Fe_{3(x)}$, x = 0.4 (blue dots)

The theoretical $\chi_M T$ value for 100% of $Fe^{II}_{HS}Fe^{II}_{LS}Fe^{II}_{HS}$ and $Fe^{II}_{HS}Fe^{II}_{HS}Fe^{II}_{HS}$ is represented by red arrows.

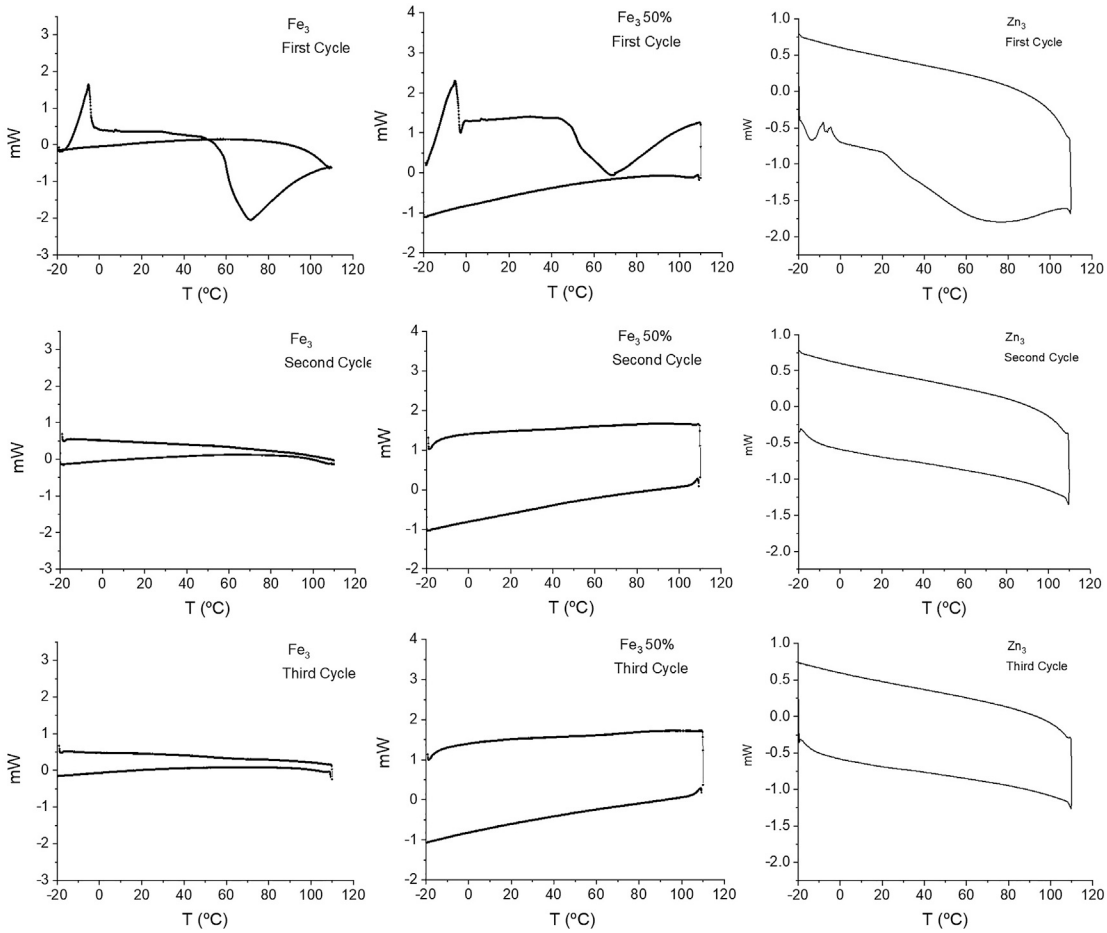

Figure 9. DSC data during successive heating/cooling cycles for (Fe_3); (Zn_3) and the solid dilution $Zn_{3(1-x)}Fe_{3(x)}$ with x = 0.5

b. These theoretical values can be determined by using this equation:

$$\chi_M T = \frac{Ng^2\mu B^2}{3k} S(S+1) \approx \frac{g^2 S(S+1)}{8}$$

Where N is the Avogadro's number ($6.022 \cdot 10^{23}$ mol^{-1}), g is the g-factor (typically g = 2 for ideal isotropic situation), k is the Boltzmann constant ($9.27 \cdot 10^{-24}$ $J \cdot T^{-1}$), μB is the Bohr magneton (5584.8 $cm^3 mol^{-1}$) and S is the total spin of the complex.

c. According to this equation, the theoretical $\chi_M T$ product for an only-spin Fe^{II}_{LS} is 0 and for an only-spin Fe^{II}_{HS} is 3 cm^3 $mol^{-1} \cdot K$, hence, the $\chi_M T$ for $Fe^{II}_{HS}Fe^{II}_{LS}Fe^{II}_{HS}$ and $Fe^{II}_{HS}Fe^{II}_{HS}Fe^{II}_{HS}$ is 6 and 9 cm^3 $mol^{-1} \cdot K$, respectively (Table 3).

d. Apply this to the experimental data: below room temperature (20°C–25°C), the experimental $\chi_M T$ value for $Zn_{3(1-x)}Fe_{3(x)}$ complexes is around 7 cm^3 $mol^{-1} \cdot K$, which corresponds to 68% of the Fe $\chi_M T$ trimers in HS-LS-HS configuration and 32% in HS-HS-HS. Upon heating up to 400K, the experimental $\chi_M T$ product increases until 9 cm^3 $mol^{-1} \cdot K$, consistent with a complete spin transition of the central Fe^{II} ion, resulting in a 100% HS-HS-HS Fe^{II} trimer in the sample, see Figure 8.

⚠ CRITICAL: In some SCO compounds, the spin transition is accompanied by a crystallographic phase transition. This phase transition can be followed by differential scanning calorimetry (DSC) and by variable temperature PXRD. In our case, we performed DSC (Figure 9) analysis and collected PXRD patterns under vacuum at different temperatures (Figure 10) to rule out the participation of a crystallographic phase transition.

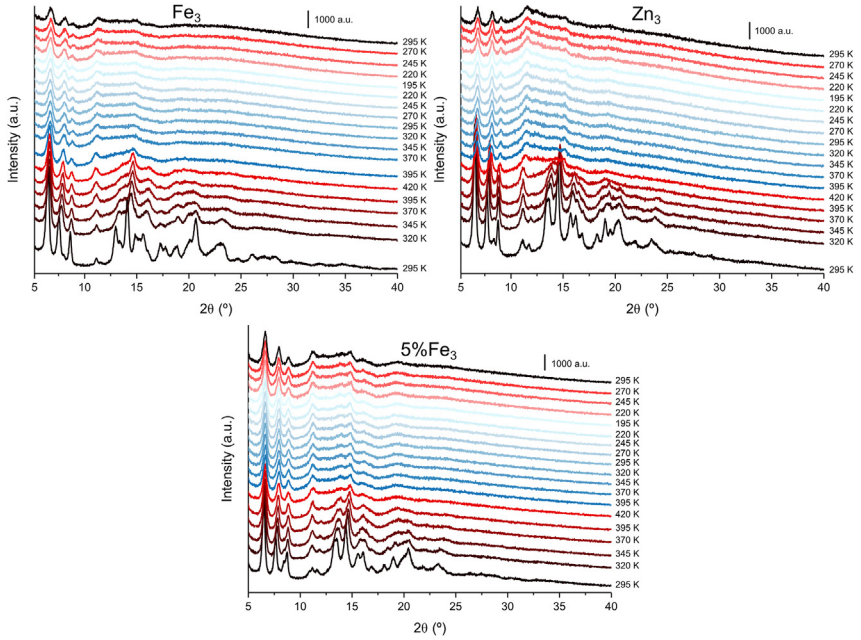

Figure 10. Evolution of powder X-ray diffraction patterns for Fe_3, Zn_3 and 5% Fe_3 during a thermal cycle between 295 K and 420 K

Note: All PXRD plots are well fitted with the crystallographic data from the **Fe_3** and **Zn_3** single-crystal solution, obtaining similar refined cell parameters in all the samples.

Note: First DSC cycle (left) shows the dehydration occurring during the first heating branch, and the absence of any feature during the first cooling branch. Second cycle (middle) does not show any sign which could be related to a phase transition. Third cycle (right) is analogous to the second one.

Spin transition detection of the polyanionic trimers in the liquid state

Timing: 3 days

The spin state transition of the **Fe_3** in liquid state is studied by NMR spectroscopy and UV-vis absorption spectroscopy.

16. Preparation of the polyanionic Fe or Zn trimers solution.
    a. Degas the water, ethylene glycol and methanol by freeze-pump-thaw cycling.
    b. Repeat 3 times this process.
    c. Dissolve the **Fe_3** powder in a specific volume of degassed water (see Table 3 for exact weight and volume).

Table 3. Summary of the theoretical $\chi_M T$ values for Fe_3 trimer

Metal ions	S	$\chi_M T$ ($cm^3 \cdot mol^{-1} \cdot K$)
Spin Only FeII (LS)	0	0
Spin-Only FeII (HS)	2	3
$Fe^{II}_{HS}Fe^{II}_{LS}Fe^{II}_{HS}$	2 + 0 + 2 = 4	3 + 0 + 3 = 6
$Fe^{II}_{HS}Fe^{II}_{HS}Fe^{II}_{HS}$	2 + 2 + 2 = 6	3 + 3 + 3 = 9

Table 4. Amount of Fe_3 and solvents for preparing Fe_3 solutions

Technique	[Fe_3]	Fe_3 weight	Organic solvent	Water
NMR	4 mM	60 mg	CD_3OD: 0.45 mL	D_2O: 0.35 mL
Evans	4 mM	60 mg	EG: 0.45 mL	D_2O: 0.35 mL
UV-vis	4 mM	225 mg	EG: 1.7 mL	H_2O: 1.3 mL

d. Once the complex is dissolved, add a specific volume of organic diluent (3:4 water:organic solvent ratio, Table 4).
e. Stir the resulting solution at room temperature (20°C–25°C).

⚠ CRITICAL: The solutions were prepared and maintained under an inert atmosphere to avoid the Fe^{II} oxidation. After the preparation, check if the solution is still colorless and without precipitation.

17. Variable temperature H-NMR spectroscopy.

Note: Variable temperature H-NMR spectroscopy can monitor the spin transition processes in solution, especially detectable in transition between Fe^{II}_{HS} (paramagnetic) and Fe^{II}_{LS} (diamagnetic) ions. In general, the paramagnetism involves fast T1 relaxation times in the protons, provoking complex H-NMR spectra with wide chemical shift range and broadened signal.

a. Prepare 4mM of **Fe_3** in D_2O: CD_3OD (3:4 v.v.), see Table 3.
b. Optimize the experimental parameters typical of paramagnetic H-NMR spectra, in our case:
   i. wide field range (SW = 100 ppm).
   ii. high scan number (128).
   iii. short d1 values (d1 = 1 s).
c. Collect the H-NMR spectra in the 200 K−300 K range.

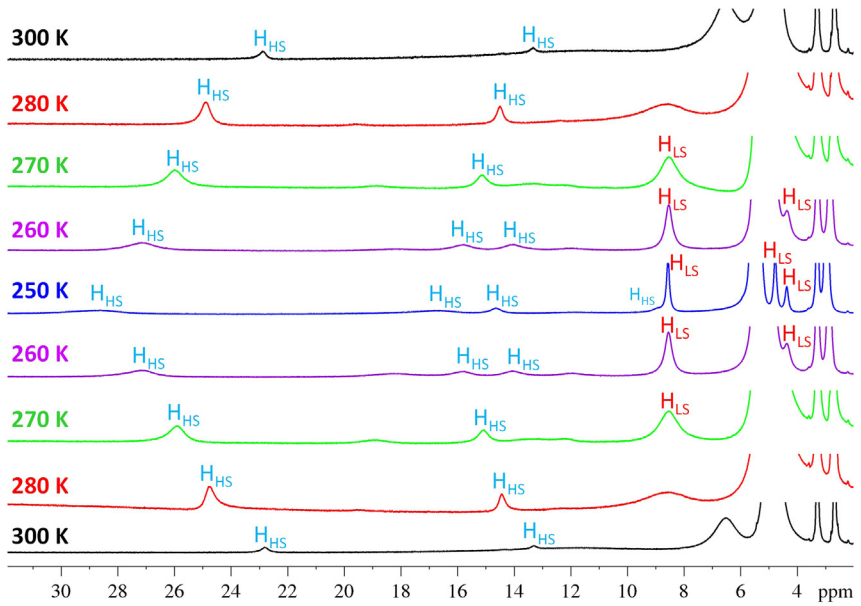

Figure 11. ^{1}H-NMR spectra of Fe_3 in D_2O:CD_3OD (3:4 v.v.) at 300–250 K temperature range
The ^{1}H signals of the HS and LS species are defined as H_{HS} and H_{LS}, respectively.

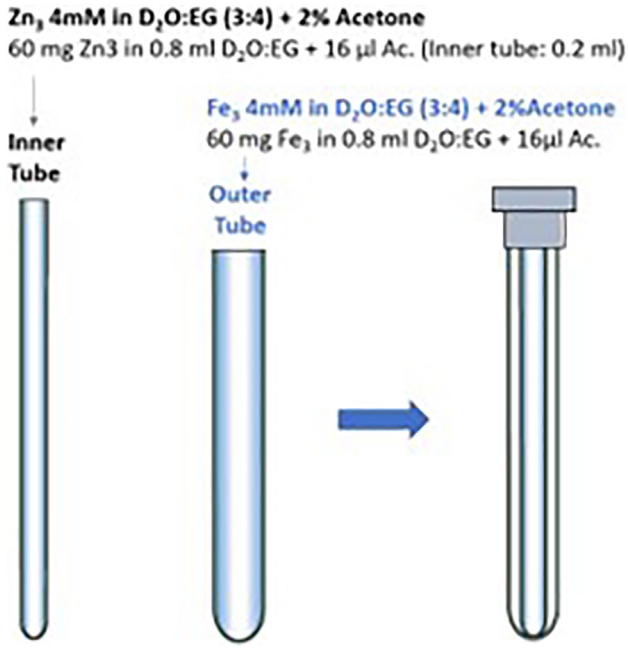

Figure 12. Sample preparation for Fe_3 spin transition characterization by Evans NMR method

d. Assign the different signals (see Figure 11):
   i. Broader and highly deshielded signals (23, 14, and 13 ppm at room temperature, 20°C–25°C) are attribute to the HS-HS-HS trimer (denoted as H_{HS}).
   ii. Sharper peaks at higher magnetic fields (8.5, 4.8, and 4.4 ppm at 250 K) are attributed to HS-LS-HS configuration (denoted as H_{LS} signals).

18. Evans NMR method.

Note: The paramagnetic susceptibility of Fe_3 in solution was determined by NMR-based Evans measurements. The Evans method estimates the total magnetic moment of the Fe_3 solution from paramagnetic shift provoked in a reference solvent (e.g. non-deuterated acetone) by the paramagnetic species.

a. Sample Preparation.
   i. Use a NMR tube with a coaxial tube insert. Fill the outer with the Fe_3 solution (4mM) in D_2O:ethylene glycol (3:4 v.v.) and the inner tube with Zn_3 solution (4mM) in D_2O:ethylene glycol (3:4 v.v.).
   ii. Add non-deuterated acetone (2% v.v) to both tubes, see Figure 12.

b. Magnetic data interpretation.
   i. Record the ^{1}H-NMR spectra in a 500 MHz spectrometer in the 250–300 K range.
   ii. Identify the inner and outer acetone signal. The inner acetone will give a H-signal at lower frequency and with lower integral (Acetone) than the outer acetone (Acetone'), Figure 13A.
   iii. Reference the inner acetone signal in all spectra at 2.05 ppm (f_1).
   iv. Measure the chemical shift in acetone signals between the inner and outer tubes (f_2-f_1).
   v. Determine the molar paramagnetic susceptibility from the experimentally measured shift in acetone signals by using this equation:

$$\chi_M = \frac{3\delta f M}{4\pi f m}$$

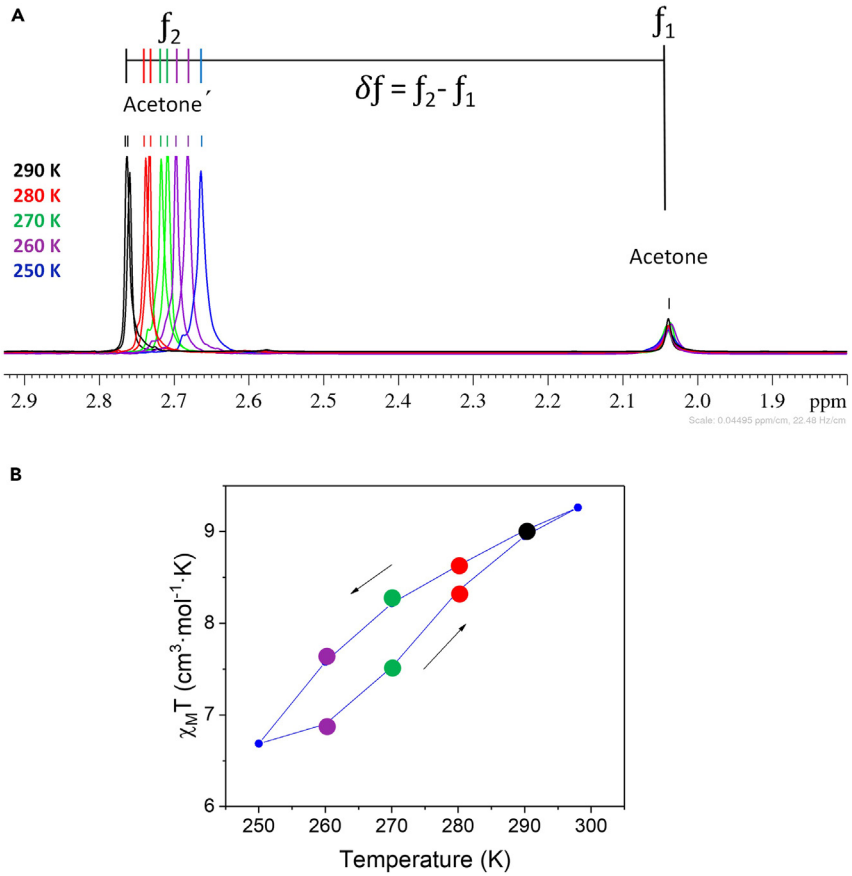

Figure 13. Evans NMR method for f Fe_3

(A) ^{1}H-NMR spectra in the 250–290 K range showing the shift in acetone ^{1}H-NMR signals between the outer (Acetone') and inner tube (Acetone).

(B) χ_M *T vs. T* graph of **Fe_3**.

where χ_M is the molar paramagnetic susceptibility (cm^3mol^{-1}), δf is the frequency difference between the acetone peaks of the inner and outer tube (f(Hz) = f(ppm)·500), M the molecular weight of the paramagnetic complex ($g \cdot mol^{-1}$), *f* the frequency of the NMR instrument (5·10 Hz) and *m* the mass of the complex (g).

vi. Plot the $\chi_M T$ *product vs. T* to obtain Figure 13B.

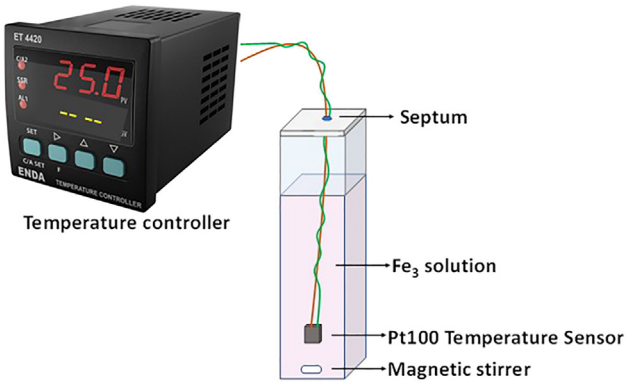

Figure 14. Representation of the set-up to read the temperature of the sample solution

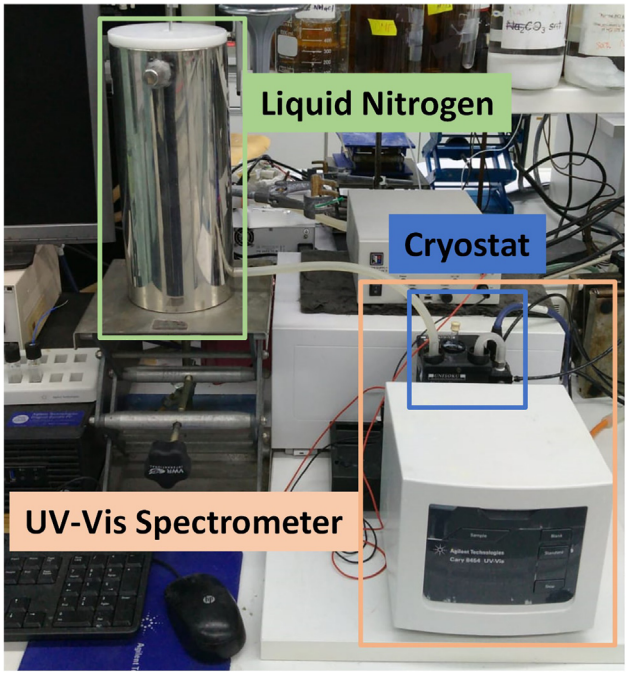

Figure 15. UV-Vis spectrometer set-up for variable temperature UV-Vis absorption measurements

Note: According to the equation $\chi_M = \frac{(3\delta f/M)}{(4\pi f m)}$, the magnetic susceptibility of Fe_3 can be estimated from this shift (δf), obtaining a $\chi_M T$ *vs* T graph.

19. UV−vis absorption.

Note: The spin transition of Fe_3 in solution can be monitored with variable temperature UV-vis spectroscopy by following the evolution of absorption band corresponding to Fe^{II} LS species.

a. Set-up preparation.

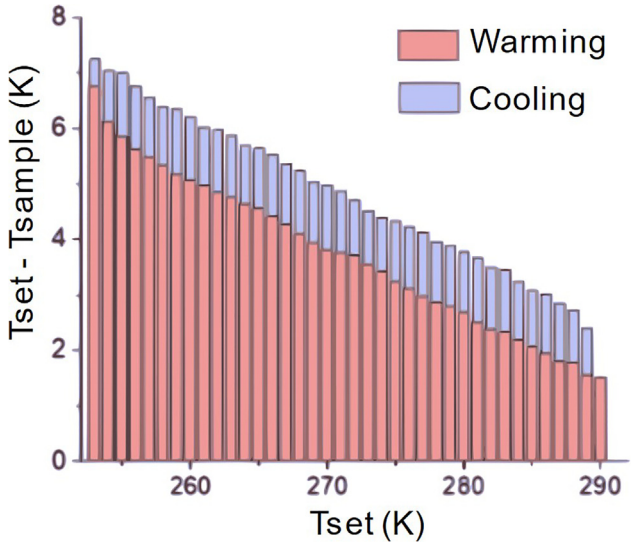

Figure 16. Difference between sample and set temperature (absolute value) during warming and cooling processes

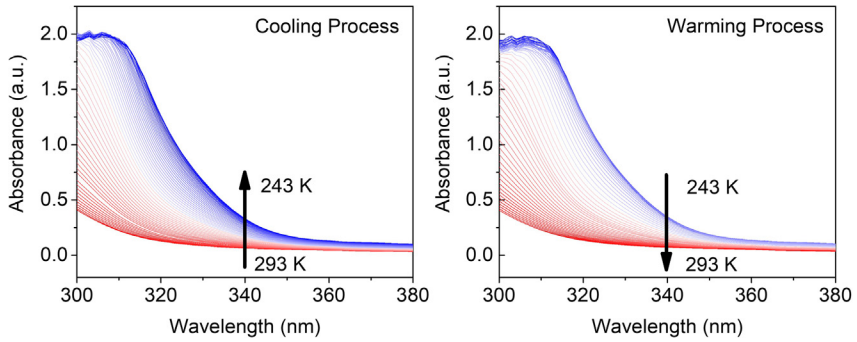

Figure 17. Temperature-dependence absorption spectra for Fe_3 solution during warming and cooling processes

i. Use a 1 cm quartz cell with a septum screw cap and introduce a magnetic stirrer.
ii. Place a thermocouple Pt100 temperature sensor across the septum cap.
iii. Seal the Pt100 wire with a septum to avoid gas leaks.
iv. Perform several vacuum-N_2 flow cycles inside the cell.
v. Introduce the Fe_3 solution in water:ethylene glycol (3:4% v.v) mixture (4mM). See section "Preparation of the polyanionic Fe or Zn trimers solution".
vi. Connect the temperature sensor to a temperature controller. See the set-up in Figure 14.
vii. Place the cell with the Pt100 in a cryostat (Unisoku Scientific Instrument).

Note: The temperature can be controlled from -80°C to 100°C by using liquid nitrogen as a coolant. This cryostat is placed inside a sample compartment of Agilent 8453 diode array spectrophotometer (l = 190–1,100 nm), see Figure 15.

viii. Set the *kinetic* mode in the spectrometer software (1 spectra·min^{-1}) and manually set the temperature in the cryostat during heating and cooling processes (0.5 K min^{-1} – 0.1 K min^{-1} range scan rate).
ix. The exact temperature in the solution was monitored by thermocouple Pt100 controller.

⚠ CRITICAL:. It is important to monitor the exact sample temperature that correspond to each spectrum to mitigate the difference between the set and sample temperature (up to

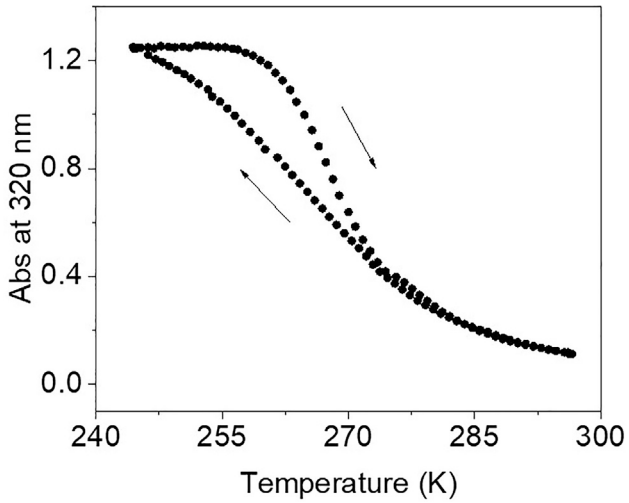

Figure 18. Thermal evolution of the absorbance at 320 nm

8 degrees at low temperature 240 K) and the different thermalization during cooling and warming processes, Figure 16.

b. UV-Vis absorption data
   i. The evolution of the absorption band around 320 nm is analyzed upon warming and cooling processes in 293-240 K range, Figure 17.
   ii. From these spectra, we plot the evolution of absorbance at 320 nm as a function of temperature in the warming and cooling branches obtaining hysteresis cycle describing the spin transition, Figure 18.

EXPECTED OUTCOMES

This protocol provides different tools and techniques for the analysis of the SCO behavior of low cooperative systems in the solid and liquid state. In the solid state, we synthesized and characterized highly diluted samples with low cooperativity between SCO centers, where upon 40–95% of the SCO active Fe^{II} was replaced by non-SCO active Zn^{II}. Magnetic measurements have been optimized to measure these samples, observing thermal hysteresis in all the diluted samples. In the liquid state, spectroscopic methods (based on NMR and UV-vis spectroscopy) were optimized to study the SCO behavior of SCO iron complex solution, a system where the cooperative intermolecular interactions are non-existent. This complex solution shows thermal hysteresis and bistability in solution by using different methods.

LIMITATIONS

The low solubility of $\mathbf{Fe_3}$ in aqueous/organic solvents represent one experimental limitation to explore the spin transition at lower temperatures than 240 K. However, optimized conditions allow us to explore enough temperature range to verify the thermal hysteresis of $\mathbf{Fe_3}$ in solution.

The visualization of a single SCO molecule at atomic resolution still represents an inherent limitation to study the spin transition of a completely isolated SCO molecule. High resolution techniques (as STM) require the deposition of the molecules on surfaces, preventing the free movement of the molecule due to the molecule-surface interaction.

TROUBLESHOOTING

Problem 1

The obtention of **L** is very sensitive to ambient humidity and temperature. When the ambient temperature and humidity is high (e.g., during summer), the product does not precipitate after the addition of ethanol to the yellow oil.

Related to step 4.

Potential solution

It is suggested to add cold ethanol to the yellow oil, which favors the fast precipitation of the product with high ambient temperature and humidity. After that, if the solution does not turn immediately cloudy, small scratches in the beaker can help to promote precipitation or crystal nucleation of the product.

Problem 2

In the samples with high concentration of diamagnetic Zn_3 (e.g., $Zn_{3(1-x)}Fe_{3(x)}$ (x = 0.05)), the resulting $\chi_M T$ *vsT* graph after the diamagnetic correction (related to step 14) show negative slope in the $\chi_M T$ *vsT* during the first heating 200–300 K range. This evidence an extra-diamagnetic contribution (Figure 7).

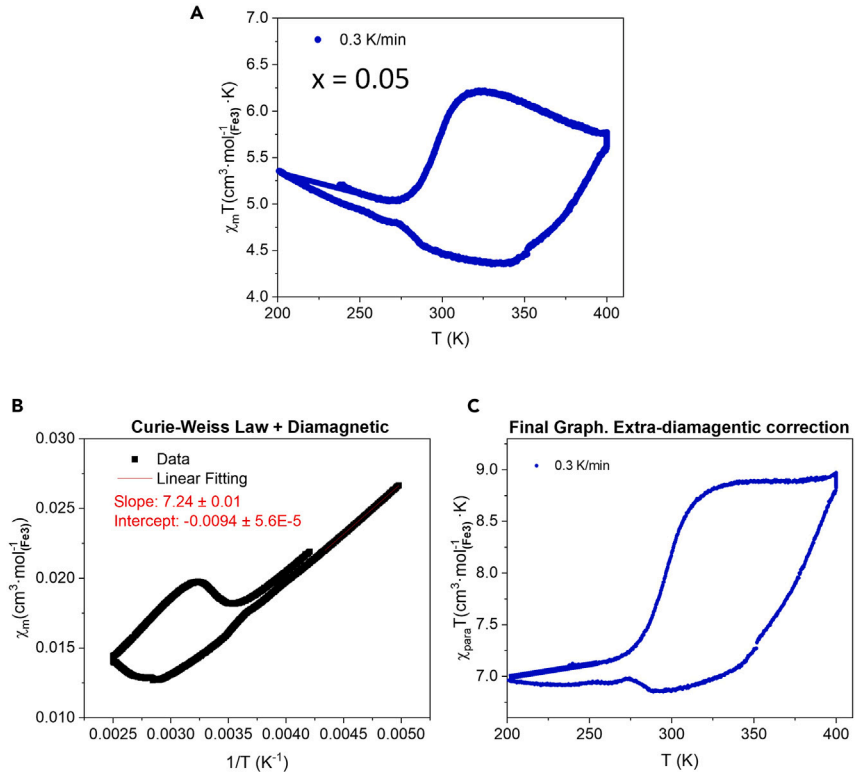

Figure 19. Data correction process for magnetic susceptibility cycle of $Zn_{3(1-x)}Fe_{3x}$ (with x = 0.05)

(A) $X_m \cdot T$ vs. T graph after standart diamagnetic correction. (B) Magnetic susceptibility vs T^{-1} and the linear fitting in low temperature range to extract the extra diamagnetic contribution from Curie Law. (C) Final graph representing the $X_{para} \cdot T$ *product vs* T.

Potential solution

In these highly diluted samples, an extra diamagnetic correction is needed: This diamagnetic contribution can be experimentally obtained by using the Curie law with addition of a diamagnetic term:

$$\chi_M = \frac{C}{T} + \chi_{DIA}$$

where χ_M is the magnetic susceptibility ($cm^3 \cdot mol^{-1}$), C is the Curie constant, T is temperature and χ_{DIA} corresponds to the diamagnetic contribution.

Then, the diamagnetic susceptibility can be empirically calculated from linear fit of χ_M *vs.* T^{-1} *plot*, where the abscissa intercept is the χ_{DIA} value, Figure 19B. The paramagnetic susceptibility (χ_{para}) are obtained by subtracting the χ_{DIA} to the χ_M value ($\chi_{para} = \chi_M - \chi_{DIA}$), Figure 19C.

Problem 3

Fe_3 and Zn_3 complexes are highly soluble in water (100 mg/mL as saturated solution) but they are not soluble in organic solvents. However, the detection of the spin conversion of Fe_3 in solution requires a wide temperature range with the lowest working temperature at 240 K or −33°C, where the Fe_3 aqueous solution is completely frozen.

Related to step 16.

Potential solution

The Fe_3 and Zn_3 were dissolved in water/ethylene glycol and water/methanol mixtures (3.4 v.v. or 57% by volume), showing freezing points around -50°C and -65°C, respectively (Figure 20).

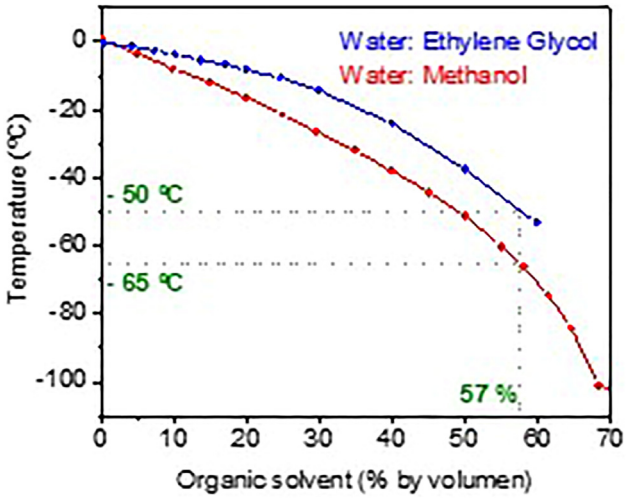

Figure 20. Freezing point of methanol and ethylene glycol aqueous solutions[18]

On the other hand, the concentration of Fe_3 and Zn_3 in aqueous-organic mixture has to be optimized to avoid precipitation. The higher concentration recommended to used is 8 mM in water/ethylene glycol and 4 mM in water/methanol.

Problem 4

Evans method requires the presence of reference acetone in the studied solution. In presence of 2% of acetone, the Fe_3 and Zn_3 precipitate below 250 K in a 4mM D_2O:CD_3OD (3:4 v.v.) mixture. Decreasing the concentration down to 1mM, the solution is stable at 250 K but the paramagnetic shift in the acetone H-NMR signal is not detectable.

Related to step 18.

Potential solution

It is recommended to use D2O:ethylene glycol (3:4 v.v.) as diluent solvent, where the Fe_3 and Zn_3 (4mM) solutions are stable even at 250 K and the spin transition can be detected in this system.

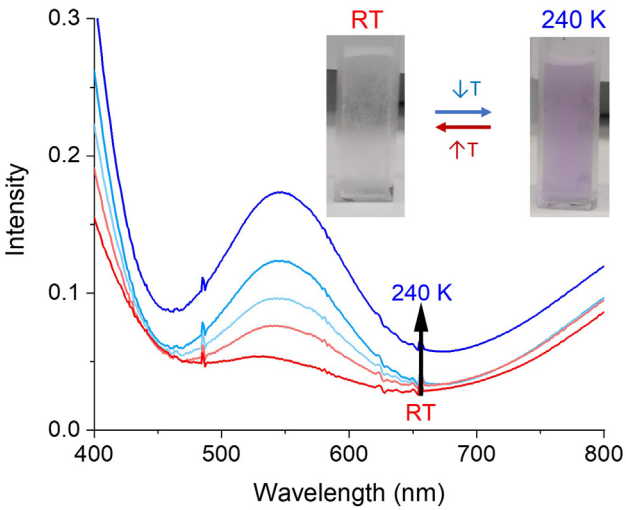

Figure 21. Temperature-dependence visible absorption spectra for Fe_3 solution (inset) Picture of Fe_3 solution at erature and at 240 K

Some parts of Figures 5, 7, 11, 13, 17, 18, 20 are from Galán-Mascaros et al. *Chem.*, 9, 377 (2022).

Problem 5

The spin transition of Fe_3 in solution is evidenced by a visible color change of the Fe_3 solution from colorless to pink and the appearance of an absorption band around 550 nm upon cooling up to 240 K, Figure 21.

Related to step 19.

However, the low absorbance intensity of this band at 240 K ($Abs_{550\ nm}$ = 0.18) is not enough to detect small spectra differences between warming and cooling processes at certain temperature.

Potential solution

We can observe higher absorbance intensity at 240 K around 320 nm and more significant temperature dependence in the 240–293 K range, Figure 17. This allows us to follow the spin transition of Fe_3 in solution, describing a hysteresis thermal cycle.

RESOURCE AVAILABILITY

Lead contact

Further information and requests for resources and reagents should be directed to and will be fulfilled by the lead contacts, Andrea Moneo Corcuera (andrea.moneo@bcmaterials.net), David Nieto Castro (dnieto@cidetec.es) and José Ramón Galán Mascarós (jrgalan@iciq.es).

Materials availability

This protocol did not generate new unique reagents.

Data and code availability

The published article includes all datasets/codes generated or analyzed during this study.

ACKNOWLEDGMENTS

This work was supported by the European Union (projects ERC StG grant CHEMCOMP no. 279313 and ERC CoG grant GREENLIGHT_REDCAT no. 648304); the Ministerio de Ciencia e Innovación for support through Severo Ochoa Excellence Accreditation 2020–2023 (CEX2019-000925-S, MIC/AEI) and Maria de Maeztu Exellence Accreditation (MDM-2017-0767); the Spanish Ministerio de Ciencia e Innovación through the projects PID2021-124796OB-I00, PGC2018-095808-B-I00, PGC2018-093863-B-C21, PID2020-112733GB-I00, PID2021-122464NB-I00, and PID2020-115165GB-I00; the Generalitat de Catalunya (2017-SGR-1406 and 2017-SGR-1277); and the CERCA Programme/Generalitat de Catalunya.

AUTHOR CONTRIBUTIONS

J.R.G.-M. proposed the concept. A.M.-C. and D.N.-C. performed experiments with the contribution of all authors. A.M.-C., D.N.-C., and J.R.G.-M. wrote the paper.

DECLARATION OF INTERESTS

The authors declare no competing interests.

REFERENCES

1. Moneo-Corcuera, A., Nieto-Castro, D., Cirera, J., Gómez, V., Sanjosé-Orduna, J., Casadevall, C., Molnár, G., Bousseksou, A., Parella, T., Martínez-Agudo, J.M., et al. (2023). Molecular memory near room temperature in an iron polyanionic complex. Chem *9*, 377–393.

2. Coryell, C.D., Stitt, F., and Pauling, L. (1937). The magnetic properties and structure of ferrihemoglobin (methemoglobin) and some of its compounds. J. Am. Chem. Soc. *59*, 633–642.

3. Gütlich, P., Hauser, A., and Spiering, H. (1994). Thermal and optical switching of iron (II) complexes. Angew. Chem. Int. Ed. Engl. *33*, 2024–2054.

4. Bousseksou, A., Molnár, G., Salmon, L., and Nicolazzi, W. (2011). Molecular spin crossover phenomenon: recent achievements and prospects. Chem. Soc. Rev. *40*, 3313–3335.

5. Stock, P., Deck, E., Hohnstein, S., Korzekwa, J., Meyer, K., Heinemann, F.W., Breher, F., and Hörner, G. (2016). Molecular spin crossover in slow motion: light-induced spin-state transitions in trigonal prismatic iron (II) complexes. Inorg. Chem. *55*, 5254–5265.

6. Ohkoshi, S.I., Imoto, K., Tsunobuchi, Y., Takano, S., and Tokoro, H. (2011). Light-induced spin-crossover magnet. Nat. Chem. *3*, 564–569.

7. Hogue, R.W., Singh, S., and Brooker, S. (2018). Spin crossover in discrete polynuclear iron (II) complexes. Chem. Soc. Rev. *47*, 7303–7338.

8. Matsumoto, T., Newton, G.N., Shiga, T., Hayami, S., Matsui, Y., Okamoto, H., Kumai, R., Murakami, Y., and Oshio, H. (2014). Programmable spin-state switching in a mixed-valence spin-crossover iron grid. Nat. Commun. *5*, 3865–3873.

9. Larionova, J., Salmon, L., Guari, Y., Tokarev, A., Molvinger, K., Molnár, G., and Bousseksou, A. (2008). Towards the ultimate size limit of the memory effect in spin-crossover solids. Angew. Chem. Int. Ed *47*, 8236–8240.

10. Koo, Y.S., and Galán-Mascarós, J.R. (2014). Spin crossover probes confer multistability to organic conducting polymers. Adv. Mater. *26*, 6785–6789.

11. Kahn, O., and Martinez, C.J. (1998). Spin-transition polymers: from molecular materials toward memory devices. Science *279*, 44–48.

12. Cruddas, J., and Powell, B.J. (2019). Spin-state ice in elastically frustrated spin-crossver materials. J. Am. Chem. Soc. *141*, 19790–19799.

13. Popa, A.I., Stoleriu, L., and Enachescu, C. (2021). Tutorial on the elastic theory of spin crossver materials. J. Appl. Phys. *129*, 131101–131125.

14. Martin, J.P., Zarembowitch, J., Dworkin, A., Haasnoot, J.G., and Codjovi, E. (1994). Solid state effects in spin transitions: influence of iron (II) dilution on the magnetic and calorimetric properties of the series [FexNi1-x (4, 4′-bis (1, 2, 4-triazole)) 2 (NCS) 2]. cntdot. H2O. Inorg. Chem. *33*, 2617–2623.

15. Ganguli, P., Guetlich, P., and Mueller, E.W. (1982). Effect of metal dilution on the spincrossover behavior in [FexM1-x (phen) 2 (NCS) 2](M= Mn, Co, Ni, Zn). Inorg. Chem. *21*, 3429–3433.

16. Corella-Ochoa, M.N., Tapia, J.B., Rubin, H.N., Lillo, V., González-Cobos, J., Núñez-Rico, J.L., Balestra, S.R.G., Almora-Barrios, N., Lledós, M., Güell-Bara, A., et al. (2019). Homochiral metal–organic frameworks for enantioselective separations in liquid chromatography. J. Am. Chem. Soc. *141*, 14306–14316.

17. Gómez, V., Sáenz de Pipaón, C., Maldonado-Illescas, P., Waerenborgh, J.C., Martin, E., Benet-Buchholz, J., and Galán-Mascarós, J.R. (2015). Easy excited-state trapping and record high T TIESST in a spin-crossover polyanionic FeII trimer. J. Am. Chem. Soc. *137*, 11924–11927.

18. Conrad, F.H., Hill, E.F., and Ballman, E.A. (1940). Freezing points of the system ethylene glycol–methanol–water. Ind. Eng. Chem. *32*, 542–543.